

V.Sorkin · E. Polturak · Joan Adler

Path-integral Monte Carlo study of phonons in the bcc phase of ^3He

Received: 1.03.2006 / Accepted: date

Abstract Using Path Integral Monte Carlo and the Maximum Entropy method, we calculate the dynamic structure factor of solid ^3He in the bcc phase at a finite temperature of $T = 1.6$ K and a molar volume of 21.5 cm^3 . From the single phonon dynamic structure factor, we obtain both the longitudinal and transverse phonon branches along the main crystalline directions, [001], [011] and [111]. Our results are compared with other theoretical predictions and available experimental data.

Keywords quantum solid · Path Integral Monte Carlo · Maximum Entropy method · phonon spectrum · solid helium

PACS 67.80.-s · 05.10.Ln · 63.20.Dj

1 Introduction

The two isotopes of solid helium, ^3He and ^4He , are the most prominent examples of quantum solids [2,3]. These isotopes display highly anharmonic dynamics: their atoms are strongly correlated, loosely bound and make large excursions to the nearest neighbor sites. The effects are especially significant in the bcc phase of solid helium.

V.Sorkin
 Physics Department, Technion - Israel Institute of Technology, Haifa, Israel, 32000
 Tel.: +972-4-8292043
 Fax: +972-4-8295755
 E-mail: phsorkin@technunix.technion.ac.il

E. Polturak
 Physics Department, Technion - Israel Institute of Technology, Haifa, Israel, 32000
 Tel.: +972-4-829-2027
 Fax: +972-4-8295755
 E-mail: emilp@physics.technion.ac.il

Joan Adler
 Physics Department, Technion - Israel Institute of Technology, Haifa, Israel, 32000
 Tel.: +972-4 829-3937
 Fax: +972-4-8295755
 E-mail: phr76ja@tx.technion.ac.il

The dynamics of solid ^4He , in particular the phonon spectrum, has been studied over years in inelastic neutron scattering experiments [4,5,6,7]. In contrast to ^4He , there are no experimental measurements of phonon spectra of ^3He (in the bcc phase) due to the large neutron absorption cross-section of this isotope. [2,8] Recently, however, the use of inelastic X-ray scattering [9,10] offers the possibility of experimentally determining the phonon branches of ^3He . In addition, new neutron scattering experiments are being planned, [11,12] which will be able to acquire data for a sufficiently long time to observe inelastic scattering. The present study has been motivated by these developments.

Strong anharmonic effects and atomic correlations make the theoretical calculation of phonon spectra of ^3He very difficult. Several theoretical methods have been developed to treat this problem: Glyde and Khanna devised a self-consistent phonon t-matrix formalism [13], Horner applied a many-body perturbation technique [14,15], and Koehler and Werthamer employed a variational approach. These theoretical calculations are based on a variational perturbative theory and implemented at zero-temperature.[2] The predictions of these models are in quantitative disagreement with each other, due to differences in the effective potentials used to evaluate phonon interactions and details of the numerical methods employed. [16]

As a complementary approach to these methods we decided to study the excitations in bcc solid helium ^3He , by performing Quantum Monte Carlo simulations at a finite temperature. We use Path Integral Monte Carlo (PIMC)[17], which is a non-perturbative numerical method, that allows, in principle, simulations of quantum systems without any assumptions beyond the Schrödinger equation. The two body interatomic He-He potential [18] is the only input for the PIMC simulations. In our study the Universal Path Integral code of Ceperley[17] was adapted to calculate the phonon branches at finite temperature. The PIMC method, in conjunction with Maximum Entropy (MaxEnt) techniques, [19] was employed to calculate the phonon spectra of liquid [20] and solid [21]

helium (^4He) at finite temperatures. The calculated phonon spectra are in good agreement with the spectra measured by inelastic neutron scattering experiments.

The results of our study include the numerical calculation of all the phonon branches of bcc ^3He at a molar volume 21.5 cm^3 . Details of our simulations are described in Sec. 2, the results of the calculations are presented in Sec. 3.

2 Method

The PIMC method used in our simulations is based on the formulation of quantum mechanics in terms of path integrals. It has been described in detail by Ceperley [17]. The method involves mapping of the quantum system of particles onto a classical model of interacting “ring polymers”, whose elements, “beads” or “time-slices”, are connected by “springs”. The method provides a direct statistical evaluation of quantum canonical averages. In addition to static properties of the system, dynamical properties can be also extracted from PIMC simulations.[17]

The object of this study is the phonon spectrum, which can be extracted from the dynamic structure factor, $S(\mathbf{q}, \omega)$. The definition of $S(\mathbf{q}, \omega)$ in terms of density fluctuations is

$$S(\mathbf{q}, \omega) = \frac{1}{2\pi n} \int_{-\infty}^{+\infty} dt e^{i\omega t} \langle \rho_{\mathbf{q}}(t) \rho_{-\mathbf{q}}(0) \rangle, \quad (1)$$

where $\hbar\mathbf{q}$ and $\hbar\omega$ are the momentum and energy (we take $\hbar = 1$), $\rho_{\mathbf{q}}$ is the Fourier transform of the density of the solid, and n is the number density. $S(\mathbf{q}, \omega)$ is usually expressed in terms of phonons, by writing $S(\mathbf{q}, \omega)$ as a sum of terms involving the excitation of a single phonon, $S_1(\mathbf{q}, \omega)$, a pair of phonons, $S_2(\mathbf{q}, \omega)$ and higher order terms which also include interference between different terms. [2,14] In most of our simulations we calculated the $S_1(\mathbf{q}, \omega)$ term. Some calculations of $S(\mathbf{q}, \omega)$ were also performed, and will be discussed below. Additional details of the method used to calculate both $S_1(\mathbf{q}, \omega)$ and $S(\mathbf{q}, \omega)$ and extract phonon spectra are described in our paper. [21]

In the simulations we used samples containing between 128 and 432 atoms. Each atom was represented by a “ring” polymer with 64 time slices. $S(\mathbf{q}, \omega)$ was calculated for values of q between 0.14 and 1 in relative lattice units (r.l.u.= $2\pi/a$, where a is the lattice parameter). The number density was set to $\rho = 0.02801 (1/\text{\AA}^3)$ and the temperature to $T=1.6 \text{ K}$. This particular temperature was chosen to compare the phonon spectrum of ^3He with those of ^4He calculated at the same temperature [21]. A perfect bcc lattice was prepared for the initial configuration. The effects of Fermi statistics are not taken into account in our simulations, which is a reasonable approximation for the solid phase at $T=1.6 \text{ K}$.

Statistical errors were estimated by running the PIMC simulations at least 10 times, with different initial conditions in each case. After each run, $S(\mathbf{q}, \omega)$ ($S_1(\mathbf{q}, \omega)$) was extracted using the MaxEnt method [19]. The phonon energy for a given \mathbf{q} was then calculated by averaging the positions of the peak of $S(\mathbf{q}, \omega)$ over the set of the simulation runs. The error bars shown in the figures below represent the standard deviation. We collected at least 10000 data points in each simulation run and re-blocked the data [21] in blocks of 100-200 points [21]. Each simulation run took about two weeks of 12 Pentium III PCs running in parallel.

A typical example of the calculated dynamic structure factor $S_1(\mathbf{q}, \omega)$ along the [011] direction is shown in Fig.1. The figure shows both the longitudinal and transverse phonons. As seen in Fig.1 the two transverse phonons have narrow and almost symmetric line shapes, while the longitudinal phonon is quite broad and asymmetric. This asymmetry exhibits itself in the form of a relatively steep rise on the low-frequency side and a more gradual decrease on the high-frequency side. Similar form of the phonon spectral function was obtained by Koehler and Werthamer [16].

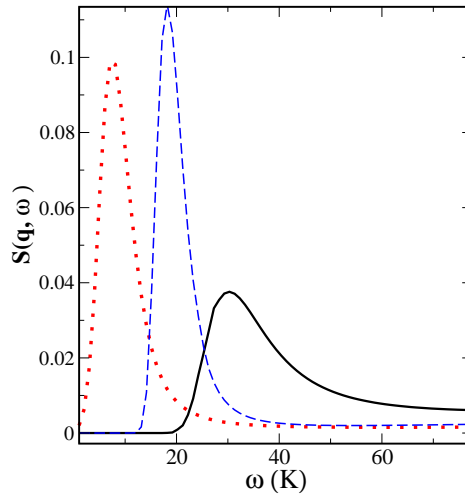


Fig. 1 Longitudinal component (solid line) and transverse components (T_1 - dotted line, T_2 - dashed line) of the dynamic structure factor, $S_1(\mathbf{q}, \omega)$, for $q = 0.4$ r.l.u. along the [011] direction.

3 Results

The calculated dispersion relations of longitudinal and transverse phonons, along the main crystal directions ([001], [111] and [011]), are shown in Figs. 2 - 7. (The numerical values are given in the Appendix).

For comparison, we plot the phonon branches calculated at $T=0 \text{ K}$ by Glyde and Khanna [13], by Koehler and Werthamer [16] (at molar volume $V=21.5 \text{ cm}^3$) and

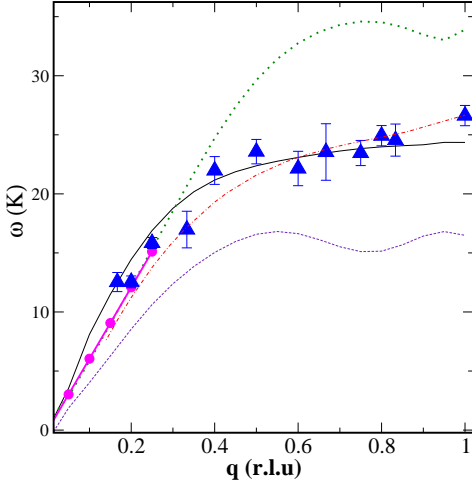


Fig. 2 Calculated dispersion relation of the L[001] phonon branch (triangles) using $S_1(\mathbf{q}, \omega)$. The error bars represent statistical uncertainty. For reference, phonon frequencies calculated by Glyde and Khanna [13] (solid lines), Koehler and Werthamer [16] (dotted lines) and Horner [15] (dashed line) are shown. The phonon spectrum at small q (circles) is estimated using elastic constants measured by Greywall [22]. The scaled single-phonon branch of ^4He (dot-dashed line) is taken from [21].

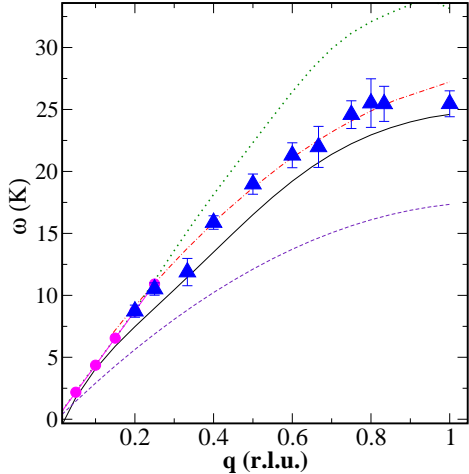


Fig. 3 Calculated dispersion relation of the T[001] phonon branch (triangles) using $S_1(\mathbf{q}, \omega)$. The error bars represent statistical uncertainty. For reference, phonon frequencies calculated by Glyde and Khanna [13] (solid lines), Koehler and Werthamer [16] (dotted lines) and Horner [15] (dashed line) are shown. The phonon spectrum at small q (circles) is estimated using elastic constants measured by Greywall [22]. The scaled single-phonon branch of ^4He (dot-dashed line) is taken from [21].

Horner [15] (at molar volume $V=24 \text{ cm}^3$). Koehler and Werthamer suggested that due to the asymmetry of the dynamic structure factor, the phonon frequency can be calculated either at the position of the maximum of $S(\mathbf{q}, \omega)$ or as the mean of the two half-maxima [16]. Since we calculated the phonon spectra using the position of the

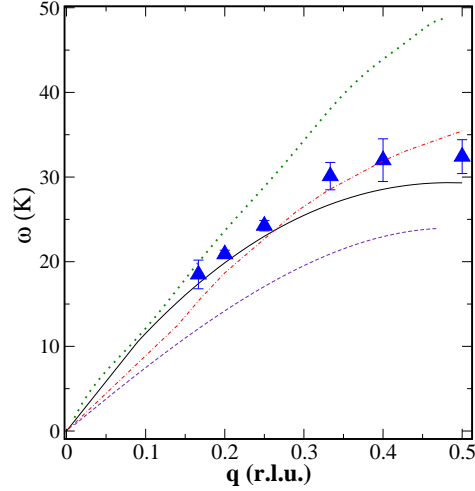


Fig. 4 Calculated dispersion relation of the L[011] phonon branch (triangles) using $S_1(\mathbf{q}, \omega)$. The error bars represent statistical uncertainty. For reference, phonon frequencies calculated by Glyde and Khanna [13] (solid lines), Koehler and Werthamer [16] (dotted lines) and Horner [15] (dashed line) are shown. The scaled single-phonon branch of ^4He (dot-dashed line) is taken from [21].

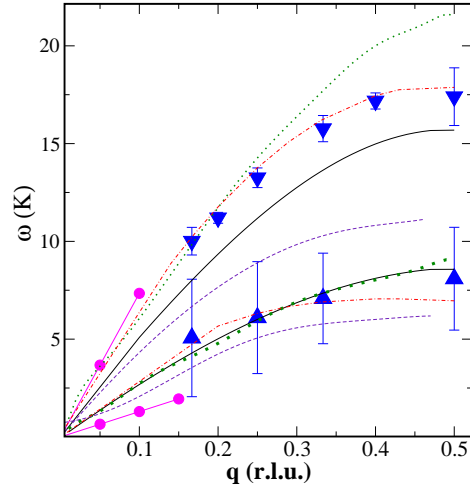


Fig. 5 Calculated dispersion relations of transverse phonon branches along [011] using $S_1(\mathbf{q}, \omega)$. Calculated values are shown for the T_1 branch (triangles down) and T_2 branch (triangles up). The error bars represent statistical uncertainty. For reference, phonon frequencies calculated by Glyde and Khanna [13] (solid lines), Koehler and Werthamer [16] (dotted lines) and Horner [15] (dashed line) are shown. The phonon spectra at small q (circles) are estimated using elastic constants measured by Greywall [22]. The scaled single-phonon branches of ^4He (dot-dashed lines) is taken from [21].

maximum of $S(\mathbf{q}, \omega)$ only these phonon frequencies were taken from Koehler and Werthamer [16].

In addition, we evaluated phonon frequencies in the long wavelength limit ($q \rightarrow 0$) using the elastic moduli of bcc ^3He measured by Greywall [22] at molar volume $V = 21.6 \text{ cm}^3$. We also made a fit to ^4He phonon branches calculated by the PIMC method [21], scaling them by

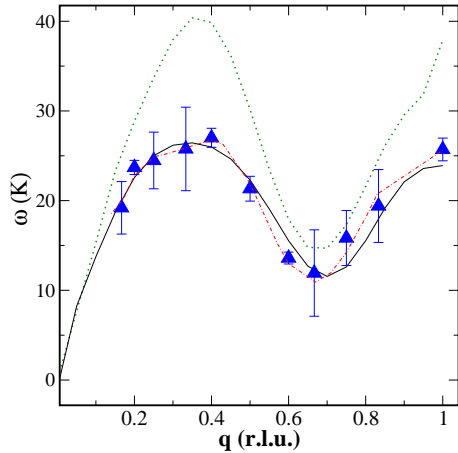


Fig. 6 Calculated dispersion relation of the L[111] phonon branch (triangles) using $S_1(\mathbf{q}, \omega)$. The error bars represent statistical uncertainty. For reference, phonon frequencies calculated by Glyde and Khanna [13] (solid lines) along with frequencies calculated by Koehler and Werthamer [16] (dotted lines) are shown. The scaled single-phonon branch of ^4He (dot-dashed line) is taken from [21].

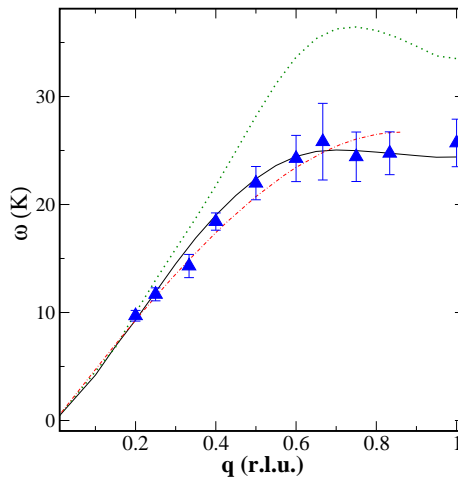


Fig. 7 Calculated dispersion relation of the T[111] phonon branch (triangles) using $S_1(\mathbf{q}, \omega)$. The error bars represent statistical uncertainty. For reference, phonon frequencies calculated by Glyde and Khanna [13] (solid lines) along with frequencies calculated by Koehler and Werthamer [16] (dotted lines) are shown. The scaled single-phonon branch of ^4He (dot-dashed line) is taken from [21].

square root of $m(^4\text{He})/m(^3\text{He})$, the mass ratio of the isotopes, and plot in Figs. 2 - 7.

Surprisingly, we found that the results of our simulations show good agreement with the theoretical calculation of Glyde and Khanna [13] (except the phonon branch T_1 [011] in Fig. 5). In addition, as can be seen from Figs. 2 - 7 the calculated phonon branches of ^3He coincide very closely with the scaled branches of ^4He (being practically on top of each other for longitudinal

phonons). We conclude that, according to our simulations, the phonon frequencies of these two isotopes scale as an inverse ratio of the square root of their atomic masses.

4 Conclusions

In conclusion, we calculated the dynamic structure factor for solid ^3He in the bcc phase of using PIMC simulations and the MaxEnt method. PIMC was used to calculate the intermediate scattering function in the imaginary time from which the dynamic structure factor was inferred with the MaxEnt method. We extracted both the longitudinal and transverse phonon branches from the one-phonon dynamic structure factor. Good agreement between the calculated phonon spectra and the theoretical prediction of Glyde and Khanna [13] has been obtained. The results of our simulations show that the phonon frequencies of these two isotopes scale as an inverse ratio of the square root of their atomic masses.

Acknowledgements We wish to thank D. Ceperley for many helpful discussions and for providing us with his UPI9CD PIMC code. We are grateful to N. Gov, O. Pelleg and S. Meni for discussions. This study was supported in part by the Israel Science Foundation and by the Technion VPR fund for promotion of research.

References

- 1.
2. H. R. Glyde, *Excitations in Liquid and Solid Helium*, Clarendon Press, Oxford, (1994).
3. E. R. Dobbs, *Solid Helium Three* (Oxford University Press, Oxford, 1994).
4. E. B. Osgood, V. J. Minkiewicz, T. A. Kitchens, and G. Shirane, *Phys. Rev. A* **5**, 1537 (1972).
5. E. B. Osgood, V. J. Minkiewicz, T. A. Kitchens, and G. Shirane, *Phys. Rev. A* **6**, 526 (1972).
6. V. J. Minkiewicz, T. A. Kitchens, G. Shirane, and E. B. Osgood, *Phys. Rev. A* **8**, 1513 (1973).
7. T. Markovich, E. Polturak, J. Bossy, and E. Farhi, *Phys. Rev. Lett.*, **88**, 195301, (2002).
8. R. Senesi, C. Andreani, D. Colognesi, A. Cunsolo and M. Nardone, *Phys. Rev. Lett.* **86**, 4584 (2001).
9. C. Seyfert, R. Simmons, H. Sinn, D. Armss and E. Burkel, *J. Cond. Matt.* **11**, 3501, (1999)
10. E. Burkel, C. Seyfert, C. Halcoussis, H. Sinn, and R. O. Simmons, *Physica B*. **263**, 412, (1999)
11. S. Schottl, K. Siemensmeyer, V. Boyko, I. Batko, S. Matias, S. Raasch, E. D. Adams, and T. E. Sherline, *J. Low Temp. Phys.*, **126**, 51, (2002)
12. R. Schanen, T. E. Sherline, A. M. Toader, V. Boyko, S. Matias, M. Meschke, S. Schottl, E. D. Adams, B. Cowan, H. Godfrin, J.P. Goff, M. Roger, J. Saunders, K. Siemensmeyer, and Y. Takano, *Physica B.*, **329**, 392, (2003)
13. H. R. Glyde and F. C. Khanna, *Can. J. Phys.*, **49**, 2997, (1971).
14. H. Horner, *J. Low. Temp. Phys.* **8**, 511, (1972).
15. H. Horner, *Phys. Rev. Lett.*, **25**, 147, (1970).
16. T. R. Koehler and N. R. Werthamer, *Phys. Rev. A*, **5**, 2230, (1972).

17. D. M. Ceperley, Rev. Mod. Phys., **67**, 279, (1995).
 18. R. A. Aziz, A. R. Janzen, and M. R. Moldover, Phys. Rev. Let. **74**, 1586 (1995).
 19. M. Jarrell and J. E. Gubernatis, Phys. Rep., **269**, 133, (1996).
 20. M. Boninsegni and D. M. Ceperley, J. Low. Temp. Phys. **104**, 336, (1996).
 21. V. Sorkin, E. Polturak and Joan Adler, Phys. Rev. B **71**, 214304 (2005)
 22. D. S. Greywall, Phys. Rev. B, **11**, 1070, (1975).

5 Appendix: Phonon energies

The energies of phonons calculated from $S_1(\mathbf{q}, \omega)$ in the bcc phase of ^4He (molar volume 21 cm^3) and ^3He (molar volume 21.5 cm^3) at $T = 1.6 \text{ K}$ are listed in Tabs. 1- 4. The phonon energy, ω , is in units of Kelvin, and the reciprocal lattice vector, q , is in relative lattice units (r.l.u.= $2\pi/a$, where $a = 4.1486 \text{ \AA}$ is the lattice parameter).

Table 1 Calculated phonon energies, $\omega(\text{K})$, of the L[001], T[001], L[111] and T[111] phonon branches of bcc ^4He obtained by using $S_1(\mathbf{q}, \omega)$.

q (r.l.u)	L[001]	T[001]	L[111]	T[111]
0.14	7.1 ± 1.9	6.1 ± 1.0	16.2 ± 1.5	6.1 ± 1.9
0.20	9.1 ± 2.5	8.1 ± 1.5	20.2 ± 2.8	8.1 ± 0.0
0.25	12.1 ± 1.5	9.1 ± 1.8	21.2 ± 2.2	10.1 ± 1.8
0.29	13.1 ± 1.6	10.1 ± 1.5	22.2 ± 4.0	10.1 ± 1.5
0.33	15.5 ± 1.4	12.1 ± 1.0	22.2 ± 1.2	13.1 ± 1.8
0.40	16.2 ± 1.6	13.1 ± 1.1	23.2 ± 2.7	15.2 ± 2.1
0.43	18.2 ± 1.5	15.2 ± 1.8	23.2 ± 3.4	16.2 ± 3.0
0.50	19.2 ± 1.1	16.2 ± 1.2	18.2 ± 1.9	18.2 ± 2.2
0.57	18.2 ± 1.4	18.2 ± 1.5	14.2 ± 4.1	20.2 ± 2.2
0.60	20.2 ± 1.7	19.2 ± 0.9	11.1 ± 2.0	20.2 ± 2.8
0.67	21.2 ± 1.7	19.2 ± 1.8	9.1 ± 2.0	22.2 ± 3.4
0.71	21.2 ± 1.9	20.2 ± 1.9	10.1 ± 1.7	22.2 ± 4.2
0.75	21.2 ± 2.2	20.2 ± 1.9	13.1 ± 1.7	21.2 ± 3.6
0.80	21.2 ± 2.2	21.2 ± 2.4	15.2 ± 1.7	22.2 ± 2.3
0.83	22.4 ± 1.7	22.5 ± 2.3	18.2 ± 1.6	24.2 ± 4.1
0.86	21.2 ± 2.6	22.2 ± 2.5	22.2 ± 1.8	23.2 ± 3.1

Table 2 Calculated phonon energies $\omega(\text{K})$ of the L[011], $T_2[011]$ and $T_1[011]$ phonon branches of bcc ^4He obtained by using $S_1(\mathbf{q}, \omega)$.

q (r.l.u)	L[011]	$T_1[011]$	$T_2[011]$
0.20	16.2 ± 2.0	5.1 ± 1.2	10.1 ± 1.3
0.25	33.3 ± 2.3	5.1 ± 1.7	12.1 ± 1.3
0.29	21.2 ± 2.7	6.0 ± 1.7	12.1 ± 1.0
0.33	26.3 ± 1.5	6.05 ± 1.1	14.2 ± 2.0
0.40	29.3 ± 1.9	6.11 ± 1.0	15.2 ± 1.5
0.43	26.3 ± 2.8	6.1 ± 1.6	16.2 ± 2.5
0.50	31.3 ± 2.5	6.12 ± 2.4	15.2 ± 1.8

Table 3 Calculated phonon energies $\omega(\text{K})$ of the L[001], T[001], L[111] and T[111] phonon branches of bcc ^3He obtained by using $S_1(\mathbf{q}, \omega)$.

q (r.l.u)	L[001]	T[001]	L[111]	T[111]
0.20	12.6 ± 0.5	8.7 ± 0.5	19.2 ± 2.9	9.7 ± 0.4
0.25	15.8 ± 0.5	10.5 ± 0.5	24.5 ± 3.1	11.7 ± 0.6
0.33	17.0 ± 1.6	11.9 ± 1.1	23.9 ± 3.9	14.3 ± 1.7
0.40	22.0 ± 1.2	15.9 ± 0.5	25.8 ± 4.7	18.4 ± 0.8
0.50	23.6 ± 0.6	18.9 ± 0.9	21.3 ± 1.1	21.9 ± 1.5
0.60	22.1 ± 1.5	21.3 ± 1.0	13.5 ± 1.5	24.7 ± 2.1
0.67	23.5 ± 2.4	22.0 ± 1.7	11.9 ± 0.7	25.8 ± 3.5
0.75	23.5 ± 1.6	24.5 ± 1.1	15.8 ± 3.1	24.3 ± 2.1
0.80	24.9 ± 0.9	25.5 ± 2.0	15.0 ± 3.6	24.7 ± 1.9
0.83	24.6 ± 1.4	25.2 ± 1.2	19.4 ± 4.1	25.2 ± 2.1
1.00	26.6 ± 0.8	25.4 ± 1.3	25.7 ± 0.7	25.7 ± 2.7

Table 4 Calculated phonon energies $\omega(\text{K})$ of the L[011], $T_2[011]$ and $T_1[011]$ phonon branches of ^3He obtained by using $S_1(\mathbf{q}, \omega)$.

q (r.l.u)	L[011]	$T_1[011]$	$T_2[011]$
0.17	18.5 ± 1.7	1.8 ± 1.5	10.0 ± 0.7
0.20	20.9 ± 0.5	2.8 ± 3.8	11.2 ± 0.3
0.25	24.2 ± 1.0	6.1 ± 2.8	13.1 ± 0.6
0.33	30.1 ± 1.6	7.1 ± 0.5	15.8 ± 0.7
0.40	32.0 ± 2.5	7.1 ± 0.0	17.2 ± 0.4
0.50	32.4 ± 2.0	8.1 ± 2.5	17.6 ± 1.1